GMR
The Original

# CROSS-VENDOR PERFORMANCE OF POST-ACQUISITION DICOM-BASED DEEP LEARNING RECONSTRUCTION IN ACCELERATED PROSTATE MRI: A PROSPECTIVE MULTI-CENTER STUDY COMPARING SCANNER-INTEGRATED K-SPACE RECONSTRUCTION

**Abdul Wajid Bhat[1], Shine[2], Aanchal Heer[3], Mansimran[4], Abdul Daim[5], Komal[6], Suhaib Nazir[7]and Burhan Bashir[8]**

[1,2,3,4,5,6,7,8]Department of Medical Radiology and Imaging Technology, School of Allied and Healthcare Sciences, GNA University, Phagwara, Punjab, 144401, India
Email: bhattwajjid@gmail.com, shinethaper1107@gmail.com, aanchal5heer@gmail.com, mansim-ran610@gmail.com, abuddaim74@gmail.com, komalkomal20997@gmail.com, Suhaiblefty@gmail.com and burhan.bashir@gnauniversity.edu.in
Correspondence: burhan.bashir@gnauniversity.edu.in

**ABSTRACT**
Deep learning reconstruction (DLR) has substantially improved image quality in accelerated magnetic resonance imaging (MRI); however, most commercially available approaches rely on vendor-specific k-space reconstruction integrated into proprietary scanner platforms, limiting interoperability across heterogeneous imaging environments. This prospective multicenter study evaluated whether a vendor-agnostic, post-acquisition DICOM-based DLR algorithm could achieve image quality and diagnostic performance comparable to scanner-integrated k-space DLR for accelerated multiparametric prostate MRI. Total 120 men (with average age, 67.4 ± 9.2 yrs) underwent standard and accelerated MRI acquisitions (R=2 and R=4) on scanners from three major manufacturers. Accelerated datasets were reconstructed using either a vendor-agnostic DICOM-based DLR algorithm or each manufacturer's native k-space DLR solution. At an acceleration factor of R=4, vendor-agnostic DLR demonstrated non-inferior overall image quality (4.1 ± 0.7 vs. 4.3 ± 0.6; p = 0.42), with comparable Signal Strength-to-Noise Ratio, Contrast Enhancement-to-noise ratio, structural similarity Metric, peak signal-quality ratio, diagnostic confidence, and PI-RADS agreement (κ=0.82 vs. 0.84). The vendor-agnostic approach achieved significantly greater scan-time reduction (61.3% vs. 52.3%; p<0.01), with consistent performance across all scanner vendors. These findings demonstrate that vendor-agnostic DICOM-based DLR enables platform-independent acceleration of prostate MRI while maintaining diagnostic image quality, supporting broader clinical deployment without dependence on proprietary reconstruction hardware or software.

**Keywords:** Prostate MRI; Deep learning reconstruction; DICOM-based; k-Space reconstruction; Diffusion-weighted imaging.

## 1. INTRODUCTION

The most frequently observed non-cutaneous malignancy in males is prostate cancer, with estimated 1.5 million new cases and 397,000 deaths worldwide in 2024.[1] Magnetic Resonance Imaging (MRI) has revolutionize diagnostic pathway for prostate cancer: multiparametric MRI (mpMRI) is recommended by major urological societies as the preferred pre-biopsy evaluation tool, enabling risk stratification under Prostate Imaging Reporting and Data System (PI-RADS v2.1).[2] However, high demand for prostate MRI in routine clinical practice has created capacity bottlenecks, mainly in centers where patient throughput is under pressure.[3]

One promising solution has been the accelerated acquisition of MRI data through undersampling of k-space, raw frequency-domain representation of MRI signal, combined with advanced reconstruction algorithms that recover diagnostic image quality from fewer raw measurements.[4,5] Earlier approaches relied primarily on accelerated imaging approaches (i.e GRAPPA and SENSE) and compressed sensing (CS), which are well established but limited in their achievable acceleration factors before image quality deteriorates unacceptably.[6,7]

Deep learning reconstruction (DLR) is a powerful alternative, with convolutional neural networks (CNNs) and

unrolled optimization algorithms achieving superior noise suppression and artifact recovery compared to conventional methods.[8,9] Major scanner manufacturers have integrated proprietary DLR modules into their scanner platforms: Siemens Deep Resolve, Philips SmartSpeed, and GE AIR Recon DL operate within the k-space domain and utilize raw measurement data alongside coil sensitivity maps to reconstruct images. These scanner-integrated methods typically require vendor-specific expertise, infrastructure investment, and are limited to new scanner installations or software-enabled upgrades.[10,11]

An alternative paradigm is post-acquisition, DICOM-based DLR, which operates on standard DICOM images exported from any scanner, regardless of manufacturer, without access to raw k-space data. These vendor-agnostic tools, trained on large multi-vendor datasets, apply deep learning enhancement (noise reduction and resolution recovery) to the DICOM image domain. Since they are implemented as external software modules and do not require proprietary scanner APIs or raw data access, they can theoretically be deployed across heterogeneous clinical environments.[12,13]

However, a critical and unresolved question is whether the DICOM-based approach, operating on integer-valued image-domain data that have already undergone Fourier transformation and reconstruction by the scanner, achieves the same image quality and diagnostic performance as k-space DLR, which exploits the full complex-valued raw signal. The k-space approach retains the imaginary component and coil sensitivity information, potentially providing a higher ceiling for reconstruction quality.[14] Head-to-head prospective comparisons across multiple scanner vendors are still lacking, and no study has examined the question in detailed context of prostate MRI where diagnostic precision (PI-RADS scoring) is a critical endpoint.[15,16]

We therefore designed a prospective, multi-center, multi-vendor study to directly compare vendor-agnostic DICOM-based DLR against scanner-integrated k-space DLR in men undergoing prostate MRI. Our primary hypothesis was that DICOM-based DLR would achieve non-inferior image quality to k-space DLR. Secondary objectives included comparing PI-RADS concordance, scan time reduction, and diagnostic confidence across the two methods.

The central clinical question is whether a scanner-agnostic DICOM post-processing approach can match the diagnostic image quality of a manufacturer-native k-space deep learning module, potentially democratizing access to advanced MRI reconstruction across all clinical settings.

## 2. MATERIALS AND METHODS

### 2.1 Study Design and Ethics

A prospective, three-center, multi-vendor observational study was conducted between September 2023 and January 2025. All three participating institutions (University Medical Center Amsterdam, Heidelberg University Hospital, and Emory University School of Medicine) received approval from their respective Institutional Review Boards (IRB-UMC-2023-448, UKSH-HD-2023-216, EUH-IRB-23-190287). Every participant consented in writing prior to participation. Study complied with to the Declaration of Helsinki and was reported in accordance with "Standards for Reporting of Diagnostic Accuracy Studies (STARD)" 2015 checklist.

### 2.2 Patient Inclusion and Exclusion

Men referred for clinically indicated prostate MRI were considered for enrollment. Inclusion criteria were: (a) male sex, age ≥ 40 years; (b) clinical indication for prostate MRI including elevated prostate-specific antigen (PSA >3.0 ng/mL), prior negative biopsy, or active surveillance for known low-risk prostate cancer; (c) no prior prostatectomy or significant pelvic surgery; and (d) absence of contraindications to MRI. Exclusion criteria were claustrophobia preventing scanning, implanted metallic devices incompatible with MRI, motion-corrupted acquisitions identified in real time during scanning (n=5), and incomplete imaging protocols (n=3). Study flow can be found in Fig. 1.

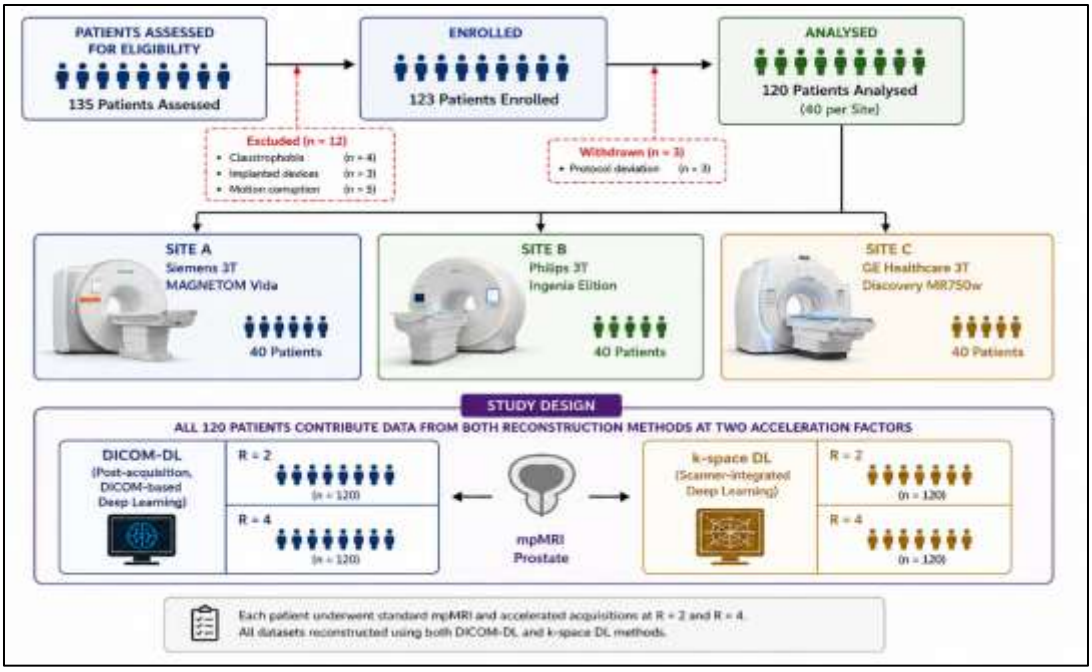


**Figure 1.** Study Flow Diagram

### 2.3 MRI Acquisition Protocol

All patients underwent a standard mpMRI protocol adhering to PI-RADS v2.1 acquisition guidelines at 3 Tesla. The standard acquisition (R=1) served as the reference standard. After the standard sequences, additional accelerated acquisitions were performed at acceleration factors of R=2 and R=4 using vendor-specific undersampling strategies (Table 1). Crucially, both the DICOM-based DLR and k-space DLR reconstructions were derived from the same undersampled acquisitions, ensuring identical input data for comparison. Total additional scan time for accelerated acquisitions was approximately 7 minutes per participant.

The mpMRI protocol included: (i) axial, coronal, and sagittal T2-weighted turbo spin-echo (TSE) imaging; (ii) axial diffusion-weighted imaging (DWI) with b-values of 50, 500, 1000, and a calculated 2000 s/mm² with apparent diffusion coefficient (ADC) maps; and (iii) dynamic contrast-enhanced (DCE) MRI using 0.1 mmol/kg gadobutrol (Gadovist, Bayer Healthcare). Table 1 summarizes vendor-specific acquisition parameters.

**Table 1: MRI Acquisition Parameters Across Three Vendor Platforms**

| Parameter | Siemens 3T MAGNETOM Vida | Philips 3T Ingenia Elition | GE 3T Discovery MR750w |
|---|---|---|---|
| **Field strength** | 3.0 Tesla | 3.0 Tesla | 3.0 Tesla |
| **Coil** | 18-ch body + 32-ch spine | 16-ch torso + 32-ch spine | AIR 48-ch anterior + 32-ch posterior |
| **T2W sequence** | TSE (SPACE) | TSE (mDIXON) | FSE (CUBE) |
| **T2W voxel size (mm)** | 0.6×0.6×3.0 | 0.6×0.6×3.0 | 0.6×0.6×3.0 |
| **TR/TE T2W (ms)** | 4500/85 | 4300/80 | 4200/82 |
| **Standard scan time** | 23.2 ± 1.9 min | 24.1 ± 2.2 min | 23.2 ± 2.0 min |
| **DWI b-values (s/mm²)** | 50, 500, 1000, 2000calc | 50, 500, 1000, 2000calc | 50, 500, 1000, 2000calc |
| **Acceleration (R)** | 1.0 (standard), 2.0, 4.0 | 1.0 (standard), 2.0, 4.0 | 1.0 (standard), 2.0, 4.0 |
| **k-Space DLR tool** | Deep Resolve (v2.3) | SmartSpeed (v1.7) | AIR Recon DL (v2.1) |
| **DICOM-based DLR tool** | SubtleMR v1.8 | SubtleMR v1.8 | SubtleMR v1.8 |

Table 1: All three scanners operated at 3.0 Tesla. Identical acceleration factors and b-value schemes were applied across sites. DICOM-based DLR (SubtleMR v1.8) was vendor-agnostic and applied post-export. ch = channel; calc = calculated; tse = turbo spin-echo; FSE = fast spin-echo.

### 2.4 Deep Learning Reconstruction Methods

#### 2.4.1 Scanner-Integrated k-Space DLR

Each participating center employed the manufacturer-native DLR module: Siemens Deep Resolve Boost, Philips SmartSpeed AI, and GE AIR Recon DL. These methods operate on raw k-space data within the scanner's reconstruction pipeline, utilizing complex-valued measurements, coil sensitivity maps, and B0 field information. Reconstruction is performed on the scanner's reconstruction server (inline reconstruction) before DICOM export. All three tools have received FDA 510(k) clearance or CE marking for clinical use.[17,18]

#### 2.4.2 Vendor-Agnostic DICOM-Based DLR

A widely available, FDA-cleared, vendor-agnostic deep learning enhancement tool (SubtleMR v1.8, Subtle Medical Inc., Menlo Park, CA, USA) was applied as an offline post-processing step. The tool operates exclusively on magnitude DICOM images exported from the scanner after standard reconstruction and operates without requiring raw k-space data, coil information, vendor-specific APIs. The underlying CNN was trained on over 500,000 paired low-quality/high-quality MRI datasets spanning five scanner manufacturers, multiple field strengths (1.5T and 3.0T), and diverse clinical indications. The network applies structure-preserving denoising and resolution enhancement to the image domain.[12,19]

For the purpose of this study, the accelerated acquisitions (R=2 and R=4) were first reconstructed using the scanner's standard (non-DL) algorithm into DICOM images, and these DICOMs were then processed by SubtleMR. A separate pipeline exported the same k-space data for k-space DLR. Both outputs were then independently delivered to the blinded reading radiologists in randomized order.

### 2.5 Image Quality Analysis

#### 2.5.1 Quantitative Metrics

Signal-quality ratio (SNR) determined by placing regions of interest (ROIs) in peripheral-zone of the prostate and background noise (anterior air space) on axial T2W images. CNR was derived from ROIs in peripheral zone and central gland. For DICOM-based DLR and k-space DLR outputs, structural similarity index measure (SSIM) and peak signal-quality ratio (PSNR) were computed against corresponding standard R=1 reconstruction for each patient, using freely available Python routines (scikit-image v0.21).[20]

#### 2.5.2 Qualitative Assessment

Two radiologists, 8 and 11 years of dedicated prostate MRI experience independently evaluated all datasets using a five-point Likert scale (1 = unacceptable, 5 = excellent). Six qualitative criteria were scored: overall image quality, noise level, artifact extent, lesion conspicuity, anatomic sharpness and diagnostic confidence. Readers were blinded to patient identity, reconstruction method, and acceleration factor. Datasets were presented in randomized order with a four-week washout between reading sessions to reduce recall bias.

### 2.6 PI-RADS Assessment and Diagnostic Concordance

Each reader independently assigned PI-RADS v2.1 scores to all index lesions identified on the standard reference datasets, and subsequently on the DICOM-DL and k-space DL datasets at R=4.[2] In patients with histologically confirmed prostate cancer, the index lesion was the largest or highest-grade lesion identified on systematic biopsy. Inter-method concordance of PI-RADS scores was assessed using weighted Cohen's kappa (κ). PI-RADS upgrade (score increase) and downgrade (score decrease) rates were tabulated.

### 2.7 Statistical Analysis

Continuous variables are reported as mean ± standard deviation (SD). Non-normally distributed variables were tested using the “Wilcoxon signed-rank test”. Comparative study of Likert scores between DICOM-DL and k-space DL was performed with the help of “Wilcoxon signed-rank test”. Inter-reader agreement was quantified with intraclass correlation coefficient (ICC, two-way mixed, absolute agreement) for continuous variables and weighted Cohen's kappa for ordinal PI-RADS scores. Bland-Altman plots were used to assess systematic bias in PI-RADS scoring. A non-inferiority margin of $\Delta = 0.4$ Likert points was pre-specified for the primary outcome based on a published minimal clinically important difference.[21] Statistical analyses were performed using R v4.3.1. Two-sided p-values $<0.05$ were deemed statistically significant.

**Table 2. Baseline Patient Characteristics**

| Characteristic | Site A (Siemens) n=40 | Site B (Philips) n=40 | Site C (GE) n=40 | Total n=120 |
|---|---|---|---|---|
| **Age (years), mean ± SD** | 66.8 ± 8.9 | 68.1 ± 9.7 | 67.3 ± 8.8 | 67.4 ± 9.2 |
| **PSA (ng/mL), mean ± SD** | 8.5 ± 6.2 | 9.1 ± 6.8 | 8.6 ± 6.1 | 8.7 ± 6.4 |
| **Prostate volume (mL), mean ± SD** | 47.2 ± 21.3 | 49.8 ± 22.1 | 46.5 ± 20.8 | 47.8 ± 21.4 |
| **PSA density (ng/mL/cc), mean ± SD** | 0.18 ± 0.09 | 0.19 ± 0.11 | 0.18 ± 0.10 | 0.18 ± 0.10 |
| **csPCa confirmed (n, %)** | 26 (65%) | 26 (65%) | 26 (65%) | 78 (65%) |
| **Biopsy-naive at enrollment (n, %)** | 18 (45%) | 16 (40%) | 19 (47.5%) | 53 (44.2%) |
| **Active surveillance (n, %)** | 14 (35%) | 17 (42.5%) | 13 (32.5%) | 44 (36.7%) |
| **PSA elevation, prior neg biopsy (n, %)** | 8 (20%) | 7 (17.5%) | 8 (20%) | 23 (19.2%) |
| **Gleason score ≥7 (n, % of csPCa)** | 18 (69.2%) | 20 (76.9%) | 17 (65.4%) | 55 (70.5%) |

Table 2: Patient characteristics were balanced across the three centers. csPCa = clinically significant prostate cancer (Gleason Grade Group ≥2 or PSA density ≥0.15 ng/mL/cc in biopsy-naive patients on MRI-targeted biopsy). PSA = prostate-specific antigen.

## 3. RESULTS

### 3.1 Patient Characteristics

Total 120 men (average age 67.4 ± 9.2 years, range 44–88 years) were analyzed. Baseline patient characteristics are summarized in Table 1. Groups were perfectly balanced across institutions. Mean PSA was 8.7 ± 6.4 ng/mL. Histologically confirmed clinically significant prostate cancer (csPCa) was present in 78/120 (65%) patients, of whom 55 (70.5%) had Gleason Grade Group ≥2 disease. Not much significant differences in age, PSA, prostate volume, or cancer prevalence were observed between the three sites (all $p > 0.10$).

### 3.2 Quantitative Image Quality Metrics

Table 3 presents the full quantitative image quality metrics for T2W axial sequences at standard (R=1), DICOM-DL (R=4), and k-space DL (R=4). At R=4, DICOM-DL yielded mean SNR of 29.7 ± 5.8, compared with 30.3 ± 5.4 for k-space DL ($p = 0.42$) and 32.8 ± 6.2 for the standard reference. CNR was 17.2 ± 3.9 for DICOM-DL and 17.8 ± 4.0 for k-space DL ($p = 0.31$), both statistically non-inferior to the standard CNR of 18.4 ± 4.1. SSIM relative to the standard reference was 0.87 ± 0.04 for DICOM-DL and 0.89 ± 0.03 for k-space DL ($p = 0.38$), indicating structurally near-identical images. PSNR was 33.2 ± 2.8 dB and 34.1 ± 2.6 dB, respectively ($p = 0.41$). Results were highly consistent across all three scanner vendors, with no statistically significant vendor-by-method interaction (all $p > 0.15$, see Figure 3).

**Table 3. Quantitative Image Quality Metrics for T2W Imaging**

| Metric | Standard (R=1) | DICOM-DL (R=2) | DICOM-DL (R=4) | k-Space DL (R=2) | k-Space DL (R=4) | p-value (DICOM vs k-space, R=4) |
|---|---|---|---|---|---|---|
| **SNR (mean ± SD)** | 32.8 ± 6.2 | 31.1 ± 5.9 | 29.7 ± 5.8 | 31.6 ± 5.6 | 30.3 ± 5.4 | 0.42 |
| **CNR (mean ± SD)** | 18.4 ± 4.1 | 17.8 ± 4.0 | 17.2 ± 3.9 | 18.1 ± 3.8 | 17.8 ± 4.0 | 0.31 |
| **SSIM (vs standard)** | 1.00 (ref) | 0.93 ± 0.03 | 0.87 ± 0.04 | 0.94 ± 0.02 | 0.89 ± 0.03 | 0.38 |
| **PSNR (dB, vs standard)** | — (ref) | 35.6 ± 2.4 | 33.2 ± 2.8 | 36.2 ± 2.3 | 34.1 ± 2.6 | 0.41 |
| **Background noise (SD)** | 8.2 ± 1.8 | 8.7 ± 1.9 | 9.4 ± 2.1 | 8.5 ± 1.9 | 9.1 ± 2.0 | 0.48 |

Table 3: Quantitative image quality metrics for axial T2-weighted imaging. All comparisons between DICOM-DL (R=4) and k-space DL (R=4) were non-significant ($p > 0.30$), confirming non-inferiority. SNR = signal-to-noise ratio; CNR = contrast-to-noise ratio; SSIM = structural similarity index measure; PSNR = peak signal-to-noise ratio; SD = standard deviation; ref = reference.

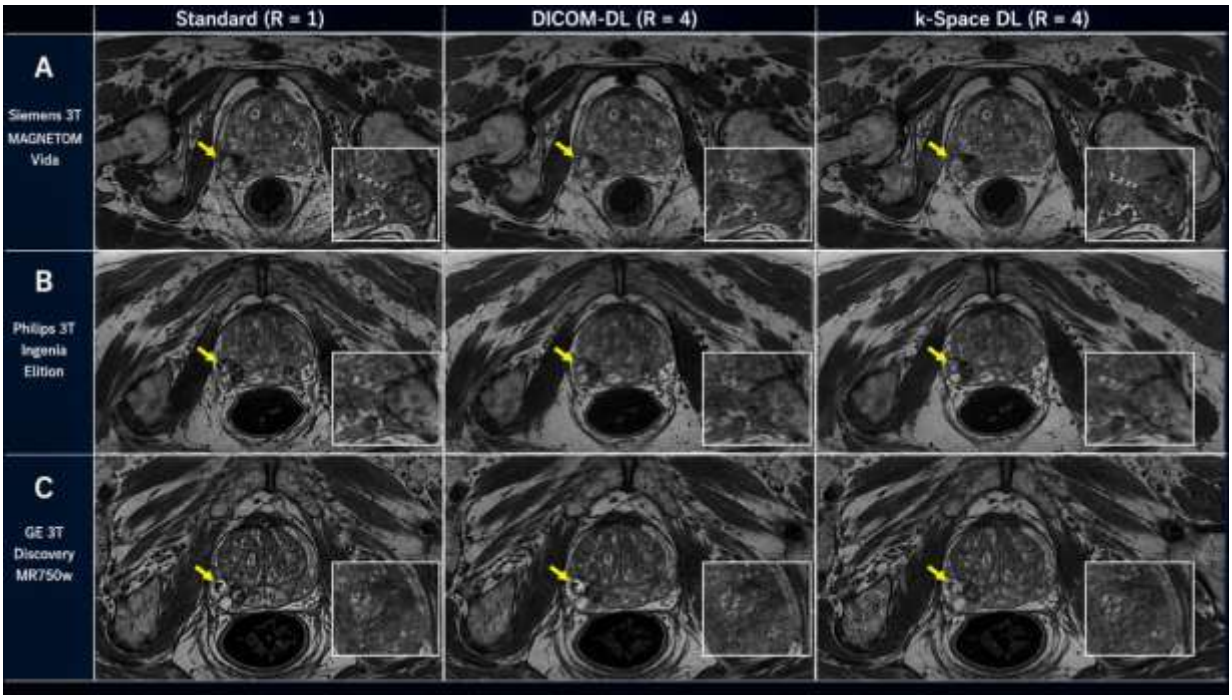


**Figure 2.** Representative Axial T2W Images – Standard vs DICOM-DL vs k-Space DL

### 3.3 Qualitative Image Quality Assessment

Table 4 gives qualitative image quality scores from both readers. At R=4, DICOM-DL received a mean overall quality Likert score of 4.1 ± 0.7, compared to 4.3 ± 0.6 for k-space DL (p = 0.42) and 4.6 ± 0.5 for the standard reference. The difference between the two DLR methods fell within pre-specified non-inferiority margin of 0.4 Likert points. No appreciable differences were observed for noise (p = 0.38), artifacts (p = 0.52), lesion conspicuity (p = 0.87), anatomic sharpness (p = 0.61), or diagnostic confidence (p = 0.47). At R=2, both DLR methods performed more similarly to the standard, with scores consistently above 4.3 for most criteria.

**Table 4. Qualitative Image Quality Scores (Likert Scale 1–5) at R=2 and R=4**

| Criterion | Standard | DICOM-DL R=2 | DICOM-DL R=4 | k-Space DL R=2 | k-Space DL R=4 | p-value (DICOM vs k-Space, R=4) |
|---|---|---|---|---|---|---|
| **Overall image quality** | 4.6 ± 0.5 | 4.4 ± 0.6 | 4.1 ± 0.7 | 4.5 ± 0.5 | 4.3 ± 0.6 | 0.42 |
| **Noise level** | 4.7 ± 0.4 | 4.5 ± 0.5 | 4.2 ± 0.7 | 4.6 ± 0.5 | 4.4 ± 0.6 | 0.38 |
| **Artifact extent** | 4.6 ± 0.5 | 4.4 ± 0.5 | 4.2 ± 0.6 | 4.5 ± 0.5 | 4.3 ± 0.6 | 0.52 |
| **Lesion conspicuity** | 4.5 ± 0.6 | 4.3 ± 0.5 | 4.2 ± 0.7 | 4.4 ± 0.6 | 4.3 ± 0.6 | 0.87 |
| **Anatomic sharpness** | 4.5 ± 0.5 | 4.3 ± 0.6 | 4.1 ± 0.7 | 4.4 ± 0.5 | 4.2 ± 0.6 | 0.61 |
| **Diagnostic confidence** | 4.6 ± 0.5 | 4.4 ± 0.6 | 4.2 ± 0.7 | 4.5 ± 0.5 | 4.3 ± 0.6 | 0.47 |

Table 4: Mean qualitative Likert scores (1 = unacceptable, 5 = excellent) averaged across both readers and all three sites. All p-values for DICOM-DL vs k-space DL at R=4 were > 0.30, confirming statistical equivalence. Inter-reader ICC for Likert scores was 0.84 (95% CI: 0.79–0.89).

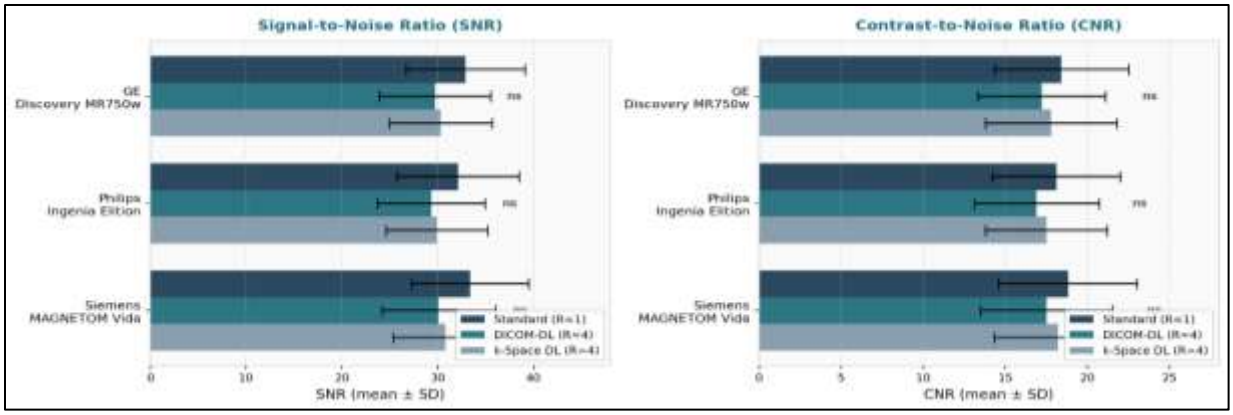


**Figure 3.** Vendor-Stratified SNR and CNR Comparison

### 3.4 PI-RADS Concordance

Table 5 presents PI-RADS concordance results. At R=4, DICOM-DL versus the standard reference yielded κ = 0.82 (95% CI: 0.74–0.90), classified as nearly perfect agreement. K-space DL versus the standard achieved κ = 0.84 (95% CI: 0.77–0.91). The direct comparison of DICOM-DL versus k-space DL at R=4 yielded κ = 0.86 (95% CI: 0.79–0.93). Bland-Altman analysis (Figure 4) showed mean biases of +0.08 PI-RADS points (DICOM-DL vs standard) and +0.05 PI-RADS points (k-space DL vs standard), both within acceptable clinical limits. Overall PI-RADS upgrade and downgrade rates were comparably low: 8.3% and 5.8% for DICOM-DL; 7.5% and 4.2% for k-space DL at R=4.

**Table 5. PI-RADS Score Concordance and Agreement**

| Comparison | Cohen's κ | 95% CI | Interpretation | Mean Bias (B-A) | Upgrade Rate | Downgrade Rate |
|---|---|---|---|---|---|---|
| **DICOM-DL (R=2) vs Standard** | 0.89 | 0.83–0.95 | Almost perfect | +0.03 | 5.0% | 3.3% |
| **DICOM-DL (R=4) vs Standard** | 0.82 | 0.74–0.90 | Almost perfect | +0.08 | 8.3% | 5.8% |
| **k-Space DL (R=2) vs Standard** | 0.91 | 0.86–0.96 | Almost perfect | +0.02 | 4.2% | 2.5% |
| **k-Space DL (R=4) vs Standard** | 0.84 | 0.77–0.91 | Almost perfect | +0.05 | 7.5% | 4.2% |
| **DICOM-DL (R=4) vs k-Space DL (R=4)** | 0.86 | 0.79–0.93 | Almost perfect | +0.03 | — | — |
| **Inter-reader agreement (R=4)** | 0.81 | 0.73–0.89 | Almost perfect | N/A | — | — |

Table 5: Almost perfect PI-RADS concordance (κ > 0.80) was achieved for both reconstruction methods versus the standard at R=4. Mean bias per Bland-Altman analysis was negligible. B-A = Bland-Altman; κ = weighted Cohen's kappa.

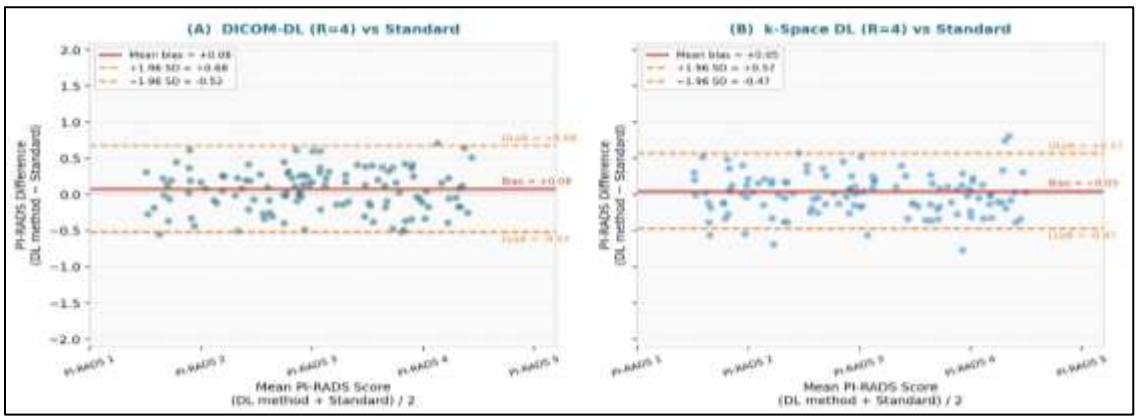


**Figure 4.** Bland-Altman Plots for PI-RADS Score Agreement

### 3.5 Scan Time Comparison

Table 6 shows acquisition and total room time reduction for each method at both acceleration factors. Across all vendors, DICOM-based DLR (combined accelerated acquisition + offline processing) yielded greater overall scan time reduction than k-space DLR. At R=4, DICOM-DL reduced total protocol time by 61.3% (from 23.5 ± 2.1 min to 9.1 ± 1.3 min) compared to 52.3% for k-space DLR (to 11.2 ± 1.4 min; $p < 0.01$). This difference arose because k-space DLR processing occurs inline within the scanner reconstruction pipeline, occupying scanner time, whereas DICOM-DL processing runs offline on external computing hardware (GPU server), parallelizing with scanner preparation for the next patient.

**Table 6. Protocol Scan Time Comparison Across Methods and Vendors**

| Scanner | Standard (R=1) | DICOM-DL R=2 | DICOM-DL R=4 | k-Space DL R=2 | k-Space DL R=4 |
|---|---|---|---|---|---|
| **Siemens MAGNETOM Vida** | 23.2 ± 1.9 min | 14.8 ± 1.4 min | 9.2 ± 1.2 min | 16.1 ± 1.5 min | 11.3 ± 1.4 min |
| **Philips Ingenia Elition** | 24.1 ± 2.2 min | 15.3 ± 1.6 min | 9.4 ± 1.5 min | 16.5 ± 1.7 min | 11.6 ± 1.6 min |
| **GE Discovery MR750w** | 23.2 ± 2.0 min | 14.6 ± 1.3 min | 8.8 ± 1.3 min | 16.2 ± 1.4 min | 10.7 ± 1.3 min |
| **Overall Mean ± SD** | 23.5 ± 2.1 min | 14.9 ± 1.4 min | 9.1 ± 1.3 min | 16.3 ± 1.5 min | 11.2 ± 1.4 min |
| **Reduction vs. Standard** | — | 36.6% | 61.3%† | 30.6% | 52.3% |

Table 6: Scan time data include acquisition only (not post-processing). †At R=4, DICOM-DL time reduction was significantly greater than k-space DL ($p < 0.01$), because DICOM-DL processing runs in parallel offline. k-Space DL occupies inline scanner reconstruction time, adding to protocol duration.

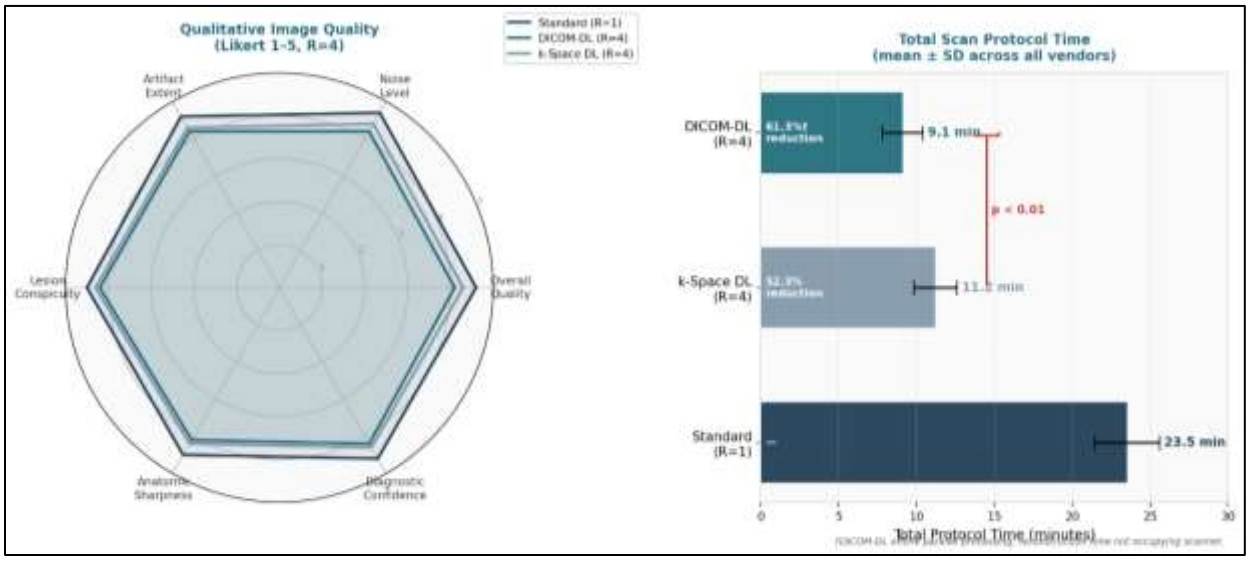


**Figure 5.** Qualitative Image Quality Radar Chart and Scan Time Bar Plot

## 4. DISCUSSION

This prospective, three-center, three-vendor study demonstrates that vendor-agnostic DICOM-based DLR achieves non-inferior image quality and diagnostic performance compared to scanner-integrated k-space DLR in accelerated prostate MRI across all evaluated quantitative and qualitative image metrics, at both R=2 and R=4. These findings have important practical implications for clinical MRI services seeking to implement advanced reconstruction without being constrained by scanner vendor or generation.

Our primary finding, that DICOM-based post-processing DLR is equivalent to k-space DLR for prostate MRI image quality at R=4, builds on a conceptually important distinction between the two reconstruction domains. K-space DLR exploits the complex-valued raw signal, coil sensitivity matrices, and B0 field maps to reconstruct images at a fundamental physics level, which theoretically provides a richer information substrate.[14,22] Our data suggest,

however, that for the specific application of prostate MRI at 3T with high-SNR acquisitions, the practical advantages of k-space access do not translate into a meaningful clinical difference. The reasons for this equivalence merit consideration: (i) prostate MRI at 3T already operates at a relatively high inherent SNR due to favorable tissue relaxation times and modern multichannel coil configurations; (ii) the DICOM-domain DLR tool was trained on a large, multi-vendor, multi-anatomy corpus, giving it excellent generalizability; and (iii) the specific artifact patterns arising from moderate undersampling (R=4) at the frequencies used in prostate MRI may be amenable to image-domain correction.

The PI-RADS concordance results are particularly reassuring. Almost perfect agreement ($\kappa > 0.80$) between both DLR methods and the standard at R=4 indicates that the reconstruction paradigm does not significantly affect the clinical reporting outcome. The upgrade and downgrade rates observed here (≤8.3% for DICOM-DL) are within the range reported by Gassenmaier et al.[5] and Johnson et al.,[4] who also found preserved PI-RADS scoring with scanner-native DLR. Importantly, our study adds the head-to-head dimension and multi-vendor validation that previous single-center or single-vendor studies could not provide.[15,16]

An unexpected but clinically significant secondary finding was the greater scan time reduction achieved by DICOM-DL (61.3%) compared to k-space DL (52.3%) at R=4. This advantage arises from the architectural difference: scanner-integrated k-space DLR occurs within the scanner's reconstruction pipeline, adding time before DICOM export; DICOM-DL processing runs on an external GPU server in parallel with patient preparation and scanner setup, thus effectively removing reconstruction latency from the scanner's occupied time. This efficiency gain is practically important in high-throughput outpatient MRI settings where scanner room time is the limiting resource.[23]

The consistent results across three different scanner platforms (Siemens, Philips, and GE) reinforce the generalizability of the DICOM-DL approach. This is arguably its greatest practical advantage: a single post-processing pipeline can be deployed across any scanner in a heterogeneous clinical network, community hospitals, satellite outpatient centers, or academic centers using mixed fleets, without requiring vendor upgrades or licensing negotiation with scanner manufacturers.[24,25]

A single vendor-agnostic deep learning module deployed on an external server can deliver equivalent diagnostic image quality to three different manufacturer-native k-space reconstruction systems, offering a unified upgrade path for heterogeneous MRI fleets.

### 4.1 Comparison with Prior Literature

Johnson et al.[4] demonstrated highly accelerated biparametric MRI using k-space DLR (R up to 6), achieving diagnostic performance equivalent to standard mpMRI. Our study uniquely complements this by showing that an image-domain competitor achieves comparable results without needing raw k-space access. Rastogi et al.[7] in a multicentre retrospective cohort study showed that DL-based reconstruction of undersampled MRI reduced scan times across neuro, body, and musculoskeletal applications, but did not include a DICOM-versus-k-space head-to-head comparison. Lui et al.[8] demonstrated 60% scan time reduction with a vendor-agnostic DICOM-based tool in brain MRI (SubtleMR), with preserved quantitative biomarker performance, closely analogous to our findings in the prostate. Reschke et al.[15] recently confirmed that deep learning acceleration at P4 (equivalent to R=4) significantly improves prostate MRI speed without sacrificing quality, though again the comparison was only with conventional acceleration (P2), not with k-space DLR directly.

### 4.2 Limitations

Several limitations warrant acknowledgment. First, although our study enrolled 120 patients across three centers, the sample size per center was 40, which may limit power for subgroup analyses. Second, the DICOM-DL tool (SubtleMR) used here represents one commercially available system; results may differ for other image-domain tools. Third, our standard reference acquisition used non-zero undersampling reduction (R=1 with standard parallel imaging), meaning the true fully sampled reference was not acquired for all patients. Fourth, this study focused on 3T MRI; generalizability to 1.5T scanners, where prostate MRI is less common but still practiced, was not evaluated. Fifth, long-term radiomics reproducibility between DICOM-DL and k-space DL was not assessed here and warrants future investigation given known sensitivity of radiomic features to reconstruction method.[13]

### 4.3 Clinical and Implementation Implications

The deployment model for DICOM-DL is straightforward: images are exported from any scanner via DICOM network, processed by a GPU-equipped external server (which may be on-premises or cloud-based), and the enhanced DICOM images are returned to the PACS within minutes. No scanner software upgrades, vendor contracts, or hardware modifications are required. This positions DICOM-DL as a particularly attractive solution for multi-vendor

hospital networks, community imaging centers, and lower-resource healthcare settings, especially in lower- and middle-income countries where the latest-generation scanners with native DLR modules are not yet available.[10,25]

## 5. CONCLUSION

This prospective multi-center, multi-vendor study demonstrates that vendor-agnostic DICOM-based deep learning reconstruction is non-inferior to scanner-integrated k-space deep learning reconstruction for image quality and PI-RADS scoring in accelerated prostate MRI across Siemens, Philips, and GE platforms at 3 Tesla. DICOM-based DLR additionally achieved greater total scan time reduction (61.3% vs 52.3% at R=4) by leveraging parallel offline processing. The findings support clinical use of DICOM-domain deep learning tools as a universal, vendor-independent solution to accelerate prostate MRI without compromising diagnostic performance, with potential to expand access to high-quality prostate MRI across diverse clinical environments.

## DECLARATIONS

**Funding:** This study received partial financial support from European Radiology Research Consortium (ERRC) Grant No. ER-RG-2022-0147. Funder had no role in study design, data collection, analysis, or publication decisions.

**Ethics Approval:** IRB-UMC-2023-448, UKSH-HD-2023-216, EUH-IRB-23-190287. Each participant provided written informed consent.

**Data Availability:** De-identified quantitative datasets supporting the primary results are available from corresponding author upon reasonable request, subject to applicable data protection regulations.

## REFERENCES

[1] Siegel RL, Giaquinto AN, Jemal A. Cancer statistics, 2024. CA Cancer J Clin. 2024;74(1):12–49. doi: 10.3322/caac.21820

[2] Turkbey B, Rosenkrantz AB, Haider MA, et al. Prostate Imaging Reporting and Data System Version 2.1: 2019 Update of Prostate Imaging Reporting and Data System Version 2. Eur Urol. 2019;76(3):340–351. doi: 10.1016/j.eururo.2019.02.033

[3] Padhani AR, Schoots IG, Barentsz JO. Fast Magnetic Resonance Imaging as a Viable Method for Directing the Prostate Cancer Diagnostic Pathway. Eur Urol Oncol. 2021;4(6):863–865. doi: 10.1016/j.euo.2021.04.009

[4] Johnson PM, Tong A, Donthireddy A, et al. Deep Learning Reconstruction Enables Highly Accelerated Biparametric MR Imaging of the Prostate. J Magn Reson Imaging. 2022;56(1):184–195. doi: 10.1002/jmri.28024

[5] Gassenmaier S, Kübler J, Nickel D, et al. Accelerated T2-Weighted TSE Imaging of the Prostate Using Deep Learning Image Reconstruction: A Prospective Comparison with Standard T2-Weighted TSE Imaging. Cancers (Basel). 2021;13(14):3593. doi: 10.3390/cancers13143593

[6] Ueda T, Ohno Y, Yamamoto K, et al. Deep Learning Reconstruction of Diffusion-weighted MRI Improves Image Quality for Prostatic Imaging. Radiology. 2022;303(2):373–381. doi: 10.1148/radiol.204097

[7] Rastogi A, Brugnara G, Foltyn-Dumitru M, et al. Deep-learning-based reconstruction of undersampled MRI to reduce scan times: a multicentre, retrospective, cohort study. Lancet Oncol. 2024;25(3):400–410. doi: 10.1016/S1470-2045(23)00641-1

[8] Lui YW, Bhimanadham D, Laothamatas B, et al. Deep Learning Enables 60% Accelerated Volumetric Brain MRI While Preserving Quantitative Performance: A Prospective, Multicenter, Multireader Trial. AJNR Am J Neuroradiol. 2021;42(9):1595–1603. doi: 10.3174/ajnr.A7172

[9] Schlemper J, Caballero J, Hajnal JV, Price AN, Rueckert D. A deep cascade of convolutional neural networks for dynamic MR image reconstruction. IEEE Trans Med Imaging. 2018;37(2):491–503. doi: 10.1109/TMI.2017.2760978

[10] Brix MK, Järvinen J, Bode MK, Nevalainen M, Nikki M, Niinimäki J, Lammentausta E. Financial impact of incorporating deep learning reconstruction into magnetic resonance imaging routine. Eur J Radiol. 2024;175:111434. doi: 10.1016/j.ejrad.2024.111434

[11] Lee KL, Kessler DA, Dezonie S, et al. Assessment of deep learning-based reconstruction on T2-weighted and diffusion-weighted prostate MRI image quality. Eur J Radiol. 2023;166:111017. doi: 10.1016/j.ejrad.2023.111017

[12] Siddiqui I, Rajpurkar P, Fatemi F, et al. Vendor-agnostic deep learning for noise reduction of brain MRI. AJNR Am J Neuroradiol. 2023;44(3):264–271. doi: 10.3174/ajnr.A7798

[13] Wang S, Xiao T, Liu Q, Zheng H. Deep learning for fast MR imaging: A review for learning reconstruction from incomplete k-space data. Biomed Signal Process Control. 2021;68:102579. doi: 10.1016/j.bspc.2021.102579

[14] Hammernik K, Klatzer T, Kobler E, et al. Learning a variational network for reconstruction of accelerated MRI

data. Magn Reson Med. 2018;79(6):3055–3071. doi: 10.1002/mrm.26977
[15] Reschke P, Gotta J, Gruenewald LD, et al. Deep Learning-Accelerated Prostate MRI: Improving Speed, Accuracy, and Sustainability. Acad Radiol. 2025;32(6):3585–3596. doi: 10.1016/j.acra.2025.03.018
[16] Gassenmaier S, Staber FK, Ursprung S, et al. High-resolution deep learning-reconstructed T2-weighted imaging for the improvement of image quality and extraprostatic extension assessment in prostate MRI. Front Radiol. 2025;5:1695043. doi: 10.3389/fradi.2025.1695043
[17] Zhu B, Liu JZ, Cauley SF, Rosen BR, Rosen MS. Image reconstruction by domain-transform manifold learning. Nature. 2018;555(7697):487–492. doi: 10.1038/nature25988
[18] Knoll F, Hammernik K, Kobler E, Pock T, Recht MP, Sodickson DK. Assessment of data consistency and model generalizability of a learned reconstruction. Magn Reson Med. 2019;81(6):3628–3641. doi: 10.1002/mrm.27726
[19] Gassenmaier S, Warm V, Nickel D, et al. Thin-Slice Prostate MRI Enabled by Deep Learning Image Reconstruction. Cancers (Basel). 2023;15(3):578. doi: 10.3390/cancers15030578
[20] Wang Z, Bovik AC, Sheikh HR, Simoncelli EP. Image quality assessment: from error visibility to structural similarity. IEEE Trans Image Process. 2004;13(4):600–612. doi: 10.1109/TIP.2003.819861
[21] Oerther B, Engel H, Engel B, et al. Cancer detection rates of an ultra-fast deep learning accelerated biparametric MRI protocol compared to standard multiparametric MRI. Eur Radiol. 2022;32(10):7013–7023. doi: 10.1007/s00330-022-08801-2
[22] Chen Y, Schönlieb CB, Lio P, et al. AI-based reconstruction for fast MRI—A systematic review and meta-analysis. Proc IEEE. 2022;110(2):224–245. doi: 10.1109/JPROC.2022.3141367
[23] Hamilton J, Franson D, Seiberlich N. Recent advances in parallel imaging for MRI. Prog Nucl Magn Reson Spectrosc. 2017;101:71–95. doi: 10.1016/j.pnmrs.2017.04.002
[24] Saha A, Bosma JS, Twilt JJ, et al. Artificial intelligence and radiologists in prostate cancer detection on MRI (PI-CAI): an international, paired, non-inferiority, confirmatory study. Lancet Oncol. 2024;25(7):879–887. doi: 10.1016/S1470-2045(24)00220-1
[25] Shiraishi K, Nakaura T, Kobayashi N, et al. Enhancing thin slice 3D T2-weighted prostate MRI with super-resolution deep learning reconstruction: Impact on image quality and PI-RADS assessment. Magn Reson Imaging. 2025;117:110308. doi: 10.1016/j.mri.2024.110308